JOURNAL OF CATALYSIS **168,** 51–59 (1997)
ARTICLE NO. CA971614

Effects of Ethanol Impregnation on the Properties of Silica-Supported Cobalt Catalysts

Sui-Wen Ho[1] and Yu-Shu Su

Department of Chemistry, National Cheng Kung University, Tainan, Taiwan 70101, Republic of China

Received May 24, 1996; revised January 2, 1997; accepted January 21, 1997

Silica-supported cobalt (6 wt%) catalysts were prepared by pore volume impregnation of either ethanol or aqueous cobalt nitrate solutions on calcined silica (500 and 1000°C), and characterized by infrared, hydrogen chemisorption, thermogravimetry–mass spectroscopy (TG-MS), and X-ray diffraction (XRD). XRD and TG show that the main cobalt phase is Co_3O_4 (above 90%) after calcination *in vacuo* to 300°C. The influence of the calcination temperature of silica on the particle size of Co_3O_4 is not significant. Smaller Co_3O_4 crystallites and more $Co{-}SiO_2$ interaction species were obtained when catalysts were prepared with ethanol instead of aqueous solution. In addition, ethoxyl groups were formed on the silica surface with a surface density of 0.17 to 0.09 ethoxyls/nm^2 depending on the calcination temperature of the pretreated silica. The decrease in Co_3O_4 crystallite size on ethanol impregnation is attributed to the presence of surface ethoxyls which might hinder the aggregation of Co_3O_4 during its formation from the thermal decomposition of cobalt nitrate. As a consequence, a larger percentage dispersion of cobalt metal was obtained after reduction at 400°C. TG-MS results showed that ethoxyl groups were decomposed into ethylene in the temperature range 500–600°C in He or H_2. Hence, ethoxyl groups might affect the sintering process of the cobalt metal during reduction as well. © 1997 Academic Press

INTRODUCTION

Cobalt is one of the most active metals for Fischer–Tropsch synthesis (1, 2). The activity and selectivity of cobalt catalysts is reported to be influenced by a number of factors, such as support (2–4), additive (6–10), and extent of cobalt reduction (11). To increase the dispersion and extent of reduction of cobalt on a inert support such as silica is of importance for studying the nature of additive or support effects without the interference of other factors. It was previously reported that impregnation with ethanolic cobalt nitrate solution instead of an aqueous one improved the dispersion of cobalt catalysts and retained a high extent of reduction of the cobalt phase (12). High activity and selectivity for gasoline and diesel fuel hydrocarbons were also reported for cobalt catalysts prepared with ethanol solution (6). Higher metal dispersion was also achieved when a dehydrated silica support was used (13). However, the nature of the ethanol effect is not well known.

The purpose of this study was to examine systematically the interaction of ethanol with silica, and the effects of ethanol impregnation and calcination temperature of pretreated silica on the dispersion and speciation of cobalt phase supported on silica after various treatments.

EXPERIMENTAL

Pretreatment of Silica

Commercial silicas (Cab-O-Sil M-5, BET surface 200 m^2/g, pore volume 1 ml/g) were impregnated with distilled water (3 ml/g) and dried at 100°C for 48 h. Dried silica powders were ground and calcined at 500°C under air flow (zero air, Sanfu, 100 ml/min) for 10 min, then calcined *in vacuo* at either 500 or 1000°C for 1 h. After cooling down to room temperature under He flow (Airproduct 99.9999%, 100 ml/min), silica powders were ready for impregnation without exposure to air.

Catalyst Preparation

Silica-supported cobalt catalysts were prepared by pore volume impregnation of the pretreated silica powders with cobalt nitrate (Alfa) solution. The solvent used was either distilled water or ethanol (absolute alcohol, RDH). The cobalt metal loading was kept at 6 wt% of the silica support. The solutions were introduced into the pretreated silica under He flow. After thorough mixing, the impregnated powders were dried under He flow at 120°C for 1 h, evacuated (<1 Torr), heated to 300°C (3°C/min), and remained at 300°C for 15 min. Catalysts were designated as CoSiXY; here X indicates calcination temperature (1000 or 500°C) of the silica support and Y, the impregnating solvent used (H for H_2O, E for ethanol). For instance, CoSi1000E represents a 6 wt% Co/SiO_2 catalyst prepared from an ethanol solution of cobalt nitrate and silica calcined at 1000°C *in vacuo*. Blank silicas were designated as SiXY. For instance, Si1000E was prepared exactly as CoSi1000E without cobalt nitrate in ethanol.

---

[1] To whom correspondence should be addressed. Fax: 886-6-2740552.

0021-9517/97 $25.00
Copyright © 1997 by Academic Press
All rights of reproduction in any form reserved.

X-ray Diffraction

A X-ray diffraction (XRD) measurements were carried out in a Shimadz XD-D1 diffractometer equipped with a graphite monochromator and scintillation detector. The X-ray tube with a copper anode was operated at 50 kV and 50 mA, and the goniometer was run at 0.01°/step with a step time of 10 s. The powdered sample was packed into a $2 \times 2 \times 0.2\text{-cm}^3$ hollowed-out slide. ASTM powder diffraction files were used to identify the phase in the sample. Crystallite sizes were calculated from line broadening using the Scherrer equation (14).

Infrared Spectroscopy

Diffuse reflectance infrared spectra were recorded on a Bomem MB100 spectrometer equipped with an *in situ* diffuse reflectance cell (Harrick) and a liquid nitrogen-cooled MCT detector. The optical path was purged with compressed air purified with Balston Drier/CO_2 Removers. The *in situ* diffuse reflectance cell can be evacuated ($<1 \times 10^{-6}$ Torr) with a turbomolecular pumping system, and heated to 600°C (sample surface temperature). Powdered samples (0.1 g) were packed into the cell and flattened with a stainless-steel spatula. Silica was used as reference material. All spectra were recorded at room temperature after various treatments.

Thermogravimetric Analysis–Mass Spectroscopy

Temperature-programmed thermal analyses were performed on a Cahn TG-121 analyzer and a VG Sensorlab 300D mass spectrometer. Through a 1.8-m heated capillary interface, the gas evolved from the thermogravimetric analyzer was analyzed with the quadrupole mass spectrometer. The pressure of the mass spectroscopy (MS) chamber is generally maintained below 5×10^{-9} Torr before sampling. The voltage for the Channeltron electron multiplier is 1575 V. In general, samples of ca. 100 mg were used. Under gas (50 ml/min) flow, the precision of the balance is within ± 1 μg. The heating rate is 10°C/min.

Hydrogen Chemisorption

Hydrogen chemisorption was performed in a conventional volumetric system evacuated by mechanical and turbo pumps. The base pressure of the system was ca. 5×10^{-6} Torr. A MKS-390 Baratron Pressure Transducer was used for pressure measurements over the range 0 to 300 Torr. Following reduction treatments, the sample was evacuated for 30 min at reduction temperature and an adsorption isotherm was taken at room temperature. The total gas uptake was determined by extrapolating the straight-line portion of the adsorption isotherm to zero pressure. The extent of cobalt reduction was determined by oxygen uptake at 400°C.

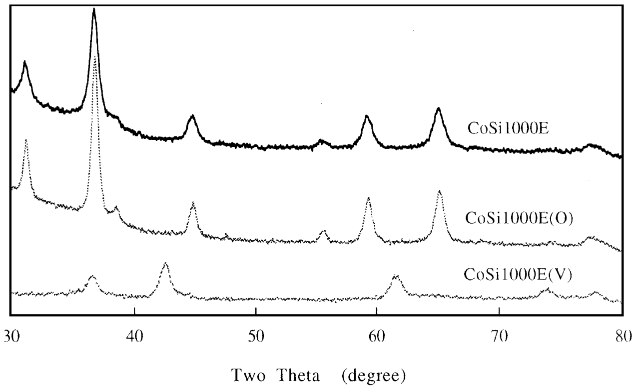

FIG. 1. X-ray powder diffraction patterns of CoSi1000E, and CoSi1000E further calcined under 1% O_2/He flow [CoSi1000E(O)] and *in vacuo* [CoSi1000E(V)].

RESULTS AND DISCUSSION

Crystalline Phase in Calcined Catalysts

The X-ray powder diffraction pattern for CoSi1000E is shown in Fig. 1. Only strong diffraction peaks characteristic of Co_3O_4 were observed that are typical of all 6% Co/SiO_2 samples calcined at 300°C *in vacuo*. This is consistent with the previous study (12). The crystallite sizes were estimated from the peak width (FWHM) of the strongest peak $\langle 311 \rangle$ ($2\theta = 36.8°$) and are given in Table 1. The Co_3O_4 crystallite sizes are smaller for CoSi500E (12 nm) and CoSi1000E (11 nm) than for CoSi500H (15 nm) and CoSi1000H (16 nm). This suggests the role that ethanol impregnation has in the aggregation of the Co_3O_4 phase during calcination. The effect of the calcination temperature of the silica support on Co_3O_4 crystallite size is not significant. The influence of ethanol impregnation on the cobalt phase on further treatments was examined by XRD. The X-ray powder diffractions of CoSi1000E further calcined to 600°C under 1% O_2/He flow [CoSi1000E(O)] and *in vacuo* [CoSi1000E(V)) are also shown in Fig. 1. For CoSi1000E(O), the diffraction peaks characteristic of Co_3O_4 remained but the peak width narrowed as a result of an increase in crystallite size to

TABLE 1

FWHM and Crystallite Size of Co_3O_4 $\langle 311 \rangle$ ($2\theta = 36.83°$) Diffraction Line

Sample	FWHM	Crystallite size (nm)
CoSi500H	0.54°	15
CoSi1000H	0.50°	16
CoSi500E	0.67°	12
CoSi1000E	0.76°	11
CoSi1000E(O)	0.57°	15

15 nm (Table 1). For CoSi1000E(V), the diffraction pattern of Co_3O_4 disappeared completely and that characteristic of CoO emerged. The same phenomena were observed for CoSi500E; however, reduction of the Co_3O_4 to the CoO phase did not occur for CoSi1000H and CoSi500H when the same treatment was applied. This suggests the presence of a reductant on CoSi1000E and CoSi500E.

Speciation and Reactivity of Ethanol Adsorbed on Silica

Some representative IR spectra of the blank silicas are shown in Fig. 2. For Si1000E, five fairly-well-resolved bands [2881 (shoulder), 2906, 2939, 2949 (shoulder), 2984 cm^{-1}] were exhibited in the region 2800–3000 cm^{-1} characteristic of C–H stretching for methyl and methylene groups. Other bands (1298, 1372, 1396, 1448, 1488 cm^{-1}) were located in the region of 1200–1500 cm^{-1}, which is characteristic of C–H bending. IR bands with the same frequency but weaker absorbance were observed for Si500E (Fig. 2). None of the above bands were found for Si1000H and Si500H. The presence of these bands indicates the formation of surface ethoxyl group ($\sim$Si–O–C_2H_5) on Si1000E and Si500E (15, 16).

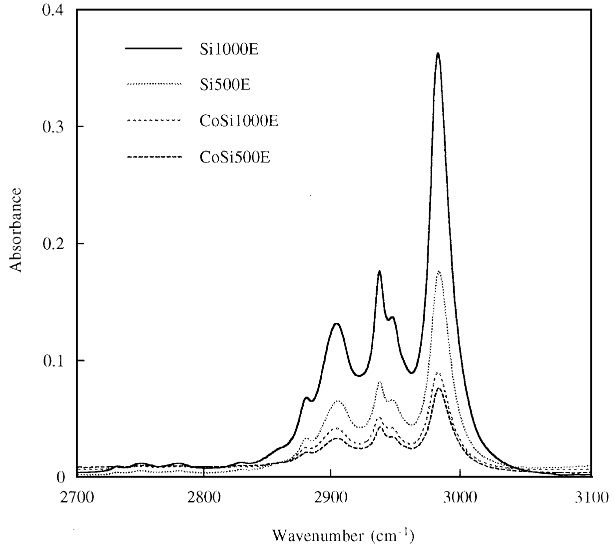

FIG. 2. Diffuse reflectance IR spectra of the ethanol-prepared SiO_2 and Co/SiO_2.

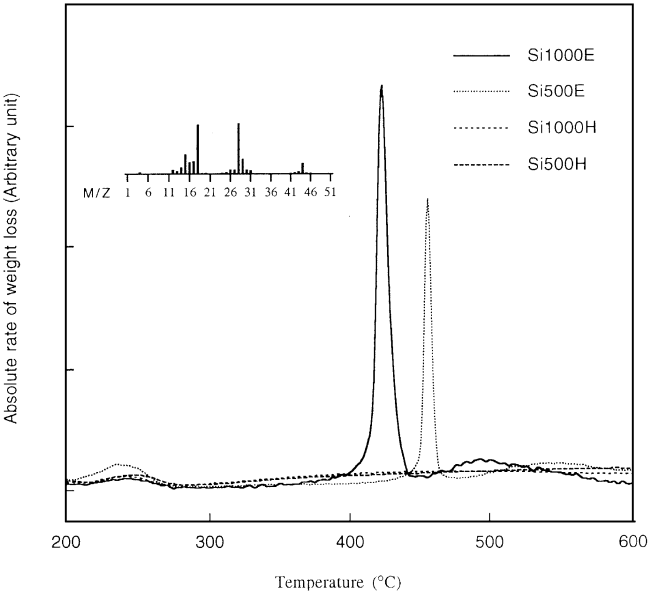

FIG. 3. DTG curves of the blank silicas obtained in 1% O_2/He flow. The inserted mass spectra was taken at the weight loss peak at 420°C in the DTG curve of Si1000E.

The thermal stability and reactivity of the ethoxyl groups on the silica surface were studied by temperature-programmed thermal analysis under oxidic, inert, and reductive atmosphere. DTG curves of the blank silicas obtained in 1% O_2/He are shown in Fig. 3. For Si1000E, one sharp peak located at 420°C and one broad band at 500°C were observed. A similar pattern of curves was obtained for Si500E, but both peak positions were about 40°C higher. Figure 3 also shows the mass spectra taken at the maximum of the weight loss peak at 420°C for Si1000E. H_2O ($m/z = 18$, 17) and CO ($m/z = 28$) were found to be the main products, with some methane ($m/z = 16, 15$), acetaldehyde ($m/z = 29$, 15, 44, 43), CO_2 ($m/z = 44$, 28), ethylene ($m/z = 28, 27, 26, 14$), ethane ($m/z = 28, 27, 26, 30, 29$), and ethanol ($m/z = 31$). Meanwhile, O_2 in the feed was consumed. This indicates that the ethoxyl groups mainly underwent oxidation in 1% O_2/He. Similar mass spectra were obtained for the 460°C peak of Si500E. The weight losses of the blank silicas under 1% O_2/He are given in Table 2. The relative weight loss ratios for the two peaks are ca. 2 : 1 (420°C : 500°C) and 1 : 1 (460°C : 550°C) for CoSi1000E and CoSi500E. To investigate if the two oxidation peaks represent different ethoxyl species, a sample of Si1000E calcined at various temperatures was monitored by IR. After calcination at 400°C in 20% O_2/He for 30 min, the absorbance of each peak decreased significantly; however, C–H stretching frequencies remained the same. Further increase in calcination temperature brought a decrease in the absorbance. Finally the peaks disappeared after calcination at 500°C for 30 min, indicating complete decomposition of the ethoxyl groups. Hence IR shows no difference in the speciation of ethoxyl groups with respect to the two oxidation peaks (420 and 500°C) on the DTG curve. The 40°C difference in oxidation temperature between Si1000E and Si500E may be due to the difference in the surface density of ethoxyl groups (shown below), where the higher the surface density, the lower the burn off temperature.

DTG curves taken in He gas flow are given in Fig. 4. A broad peak located at ca. 550°C was obtained for both Si500E and Si1000E. The weight loss is comparable to the corresponding sum of the weight losses from the two

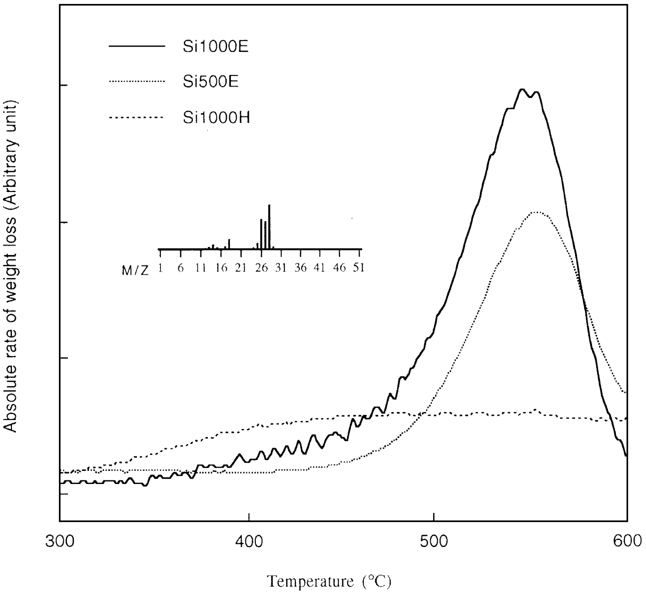

FIG. 4. DTG curves of the blank silicas obtained in He flow. The inserted mass spectra was taken at the weight loss peak at 550°C in the DTG curve of Si1000E.

oxidation peaks under 1% O_2/He flow (Table 2), indicating that complete removal of the ethoxyl groups on silica is achievable even in an inert atmosphere. In addition, mass spectra showed the formation of ethylene ($m/z = 28$, 27, 26, 14) and water in the gas phase under the weight loss peak at 550°C (inset in Fig. 4), possibly via a dehydration mechanism (17).

DTG curves and weight losses (Table 2) in H_2 flow similar to those in He flow were obtained for Si1000E and Si500E. The weight losses at 550°C were due mainly to the formation of ethylene and water.

The weight losses due to the decomposition of the ethoxyl groups in various gas flows are quite constant and average 0.78 ± 0.02 and 0.53 ± 0.03% for Si1000E and Si500E, respectively. These values correspond to surface densities of 0.5 and 0.34 ethoxyls/nm^2. The surface densities of hydroxyl groups for fully hydroxylated silica, silica calcined at 500°C *in vacuo*, and silica calcined at 1000°C *in vacuo* were reported to be 4.9, 1.8, and 0.25 OH/nm^2, respectively (18). Because the ethoxyl surface density on Si1000E was twice the reported value for hydroxyl surface density, at least half of the surface ethoxylation took place on siloxane bridges. It is likely that ethanol reacts primarily with the strained siloxane bridges, which are quite active toward forming ethoxyl group (19). This is reflected by the higher ethoxyl density obtained on Si1000E than on Si500E. Assume that all ethoxylation occurred on siloxane bridges; the proportion of siloxane bonds that reacted with ethanol to form ethoxyl groups was estimated to be ca. 20% for both Si500E and Si1000E.

TABLE 2

Weight Losses of Variously Pretreated Silica during Calcination under Various Gas Flows to 600°C

	Weight loss (%)		
Sample	1% O_2/He	He	H_2
Si1000E	0.49 (420°C)[a] 0.27 (500°C)[a]	0.78 (550°C)[a]	0.80 (540°C)[a]
Si500E	0.26 (460°C)[a] 0.30 (550°C)[a]	0.52 (550°C)[a]	0.51 (540°C)[a]
Si1000H	0.64	0.63	0.60
Si500H	0.70		0.69

[a] Temperature at which weight loss peak located.

The DTG curves of Si1000H and Si500H were generally featureless in contrast to their counterparts. The total weight loss was 0.62% for Si1000H and 0.7% for Si500H, regardless of the feed gas, and was accompanied by water formation as a result of the dehydroxylation of the silica surface (19).

Speciation and Reactivity of Ethanol Adsorbed on Calcined Co/SiO$_2$

Figure 2 also shows the diffuse reflectance infrared spectra of CoSi1000E and CoSi500E. The same vibration bands as for Si1000E and Si500E but with weaker absorbance were observed for CoSi1000E and CoSi500E, indicating the presence of ethoxyl groups on CoSi1000E and CoSi500E as well.

The DTG curves of the Co/SiO_2 catalysts in 1% O_2/He flow are shown in Fig. 5. A broad peak located at 530°C which resembled the second peak of Si500E (Fig. 3) was

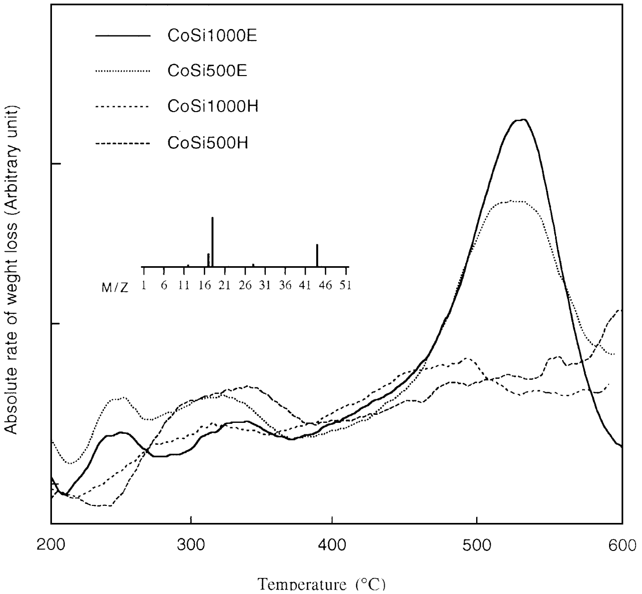

FIG. 5. DTG curves of the Co/SiO_2 catalysts obtained in 1% O_2/He flow. The inserted mass spectra was taken at the weight loss peak at 530°C in the DTG curve of CoSi1000E.

TABLE 3

Weight Losses for Various 6% Co/SiO_2 during Heating to 600°C under 1% O_2/He and He Flow

Sample	Weight loss (%)		Difference[a]
	1% O_2/He	He	
CoSi1000E	0.55 (0.25)[b] (530°C)[c]	1.25 (535–565°C)[c]	0.7
CoSi500E	0.50 (0.13)[b] (525°C)[c]	1.00 (550°C)[c]	0.5
CoSi1000H	0.87[d]	0.82[d]	−0.05
CoSi500H	0.87[d]	0.87[d]	0

[a] Differences between weight losses in He flow and weight losses in 1% O_2/He flow.

[b] Weight loss corrected for dehydration. Since the dehydration (or dehydroxylation) properties were quite similar between CoSi1000E and CoSi1000H and between CoSi500E and CoSi500H, the portion of weight loss due to dehydration around 530°C peaks for CoSi1000E and CoSi500E can be estimated from the weight loss of CoSi1000H and CoSi500H in the corresponding temperature range.

[c] Temperature at which weight loss peak located.

[d] Weight loss due to dehydration.

observed for both CoSi500E and CoSi1000E. Mass spectra show the formation of H_2O and CO_2 ($m/z = 44, 28, 12$) (inset in Fig. 5) and the consumption of O_2. The complete oxidation of ethoxyl groups to CO_2 instead of CO is expected, since Co_3O_4 is known as a good oxidation catalyst for hydrocarbons and CO (20, 21). It is likely that CO was produced initially during oxidation of the ethoxyl groups on CoSi1000E and CoSi500E, as observed for Si1000E and Si500E, and was catalytically oxidized to CO_2 on Co_3O_4 afterward. The weight losses corrected for dehydration are 0.25 and 0.13% (Table 3), which correspond to surface densities of 0.17 and 0.09 ethoxyls/nm^2 for CoSi1000E and CoSi500E, respectively. These surface densities are lower than those of the corresponding silicas suggesting possible blocking of the active siloxane bridges by cobalt species. The higher density observed for CoSi1000E is also in agreement with the assumption that ethoxylation occurred on the strained siloxane bridges. It is also noted that a small weight loss peak located at ca. 240°C is present in the DTG curves of CoSi1000E and CoSi500E (Fig. 5). A corresponding peak is also present on the mass thermograms of CO_2 for CoSi1000E and CoSi500E, but not on that for Si1000E, Si500E, CoSi1000H, and CoSi500H. Methanol was reported to be adsorbed dissociatively on Co_3O_4 surface forming methoxyl groups (22). Hence, this peak may be due to the oxidation of ethoxyl groups or other carbon species derived from ethanol on the surface of Co_3O_4 that was not detected or distinguished by IR.

DTG curves for the Co/SiO_2 catalysts under He flow are shown in Fig. 6. For CoSi500E, a broad peak located at 550°C is again observed, and the weight loss (1%) is twice that under 1% O_2/He flow (Table 3). Mass spectra show the formation of H_2O, C_2H_4 (minor), and CO_2, indicating that the weight loss originated from the oxidation of ethoxyl groups. For CoSi1000E, two close bands at 525 and 565°C are observed. The weight loss was also more than twice that obtained under 1% O_2/He flow (Table 3). For the weight loss peak at 525°C and the valley, H_2O, C_2H_4 (minor), and CO_2 were also observed in the mass spectra (insets a and b in Fig. 6), similar to that for CoSi500E; however, H_2O, CO, and CO_2 are the main products for the weight loss peak at 565°C (inset c). What happened may be rationalized as follows. The ethylene observed in the gas phase may come from the decomposition of ethoxyl groups on silica by a mechanism that is the same as that for Si1000E and Si500E. Most of the ethylene reacted with Co_3O_4 to form H_2O and CO_2; meanwhile Co_3O_4 was reduced to a lower oxidation state and an increase in weight loss was observed. This is in accordance with the XRD results that reduction of Co_3O_4 to CoO occurred on CoSi1000E and CoSi500E after calcination at 600°C *in vacuo*. If so, the extent of reduction of Co_3O_4 can be estimated from the weight losses. The differences in weight losses between that in He flow and that in 1% O_2/He flow are given in Table 3. Extra weight losses of 0.5 and 0.7% were found for CoSi500E and CoSi1000E, respectively (these values also agree very well with the differences between the weight gain on reoxidation at 400°C and the weight loss on reduction given in Table 6), and were attributed to the weight change caused by reduction of Co_3O_4 to CoO. The theoretical weight loss for complete reduction of Co_3O_4 to CoO in 6 wt% Co/SiO_2 is 0.5%. Therefore, TG indicates complete reduction of Co_3O_4 to CoO in CoSi500E, consistent with the XRD results. Since the extra

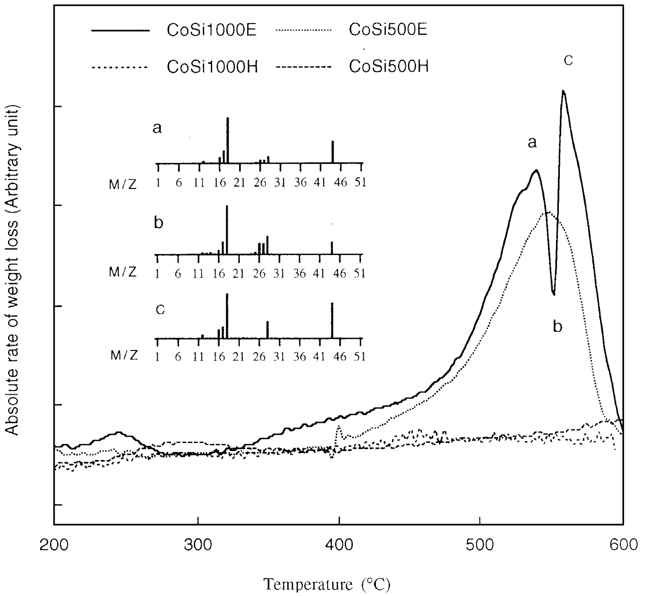

FIG. 6. DTG curves of the Co/SiO_2 catalysts obtained in He flow. The inserted mass spectra were taken at the indicated a, b, and c positions on the DTG curve of CoSi1000E.

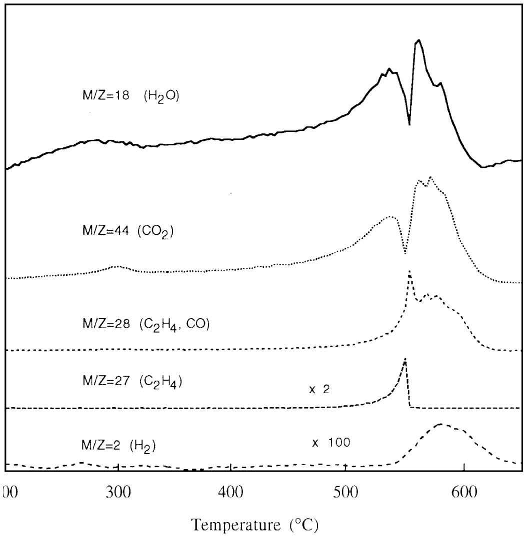

FIG. 7. Selected mass thermograms of CoSi1000E obtained in He flow.

value was higher than the theoretical one for CoSi1000E, a further reduction into zero valence state was assumed in the calculation, giving 86% CoO and 14% Co. The formation of cobalt metal may be relevant to the observed doublet in the DTG curve under He flow for CoSi1000E. Likewise, a doublet was also observed in the mass thermograms of CO_2 and H_2O for CoSi1000E (Fig. 7). In addition, a sharp peak of ethylene ($m/z = 28, 27, 26$) arose in the exact position of the valley, and bands of CO ($m/z = 28$) and H_2 ($m/z = 2$) emerged in the weight loss peak at 565°C. These results may be explained by the two-stage reduction characteristic of Co_3O_4 (23). A number of reactions occurred that could be described by the following unbalanced equations:

$$Co_3O_4 + C_2H_4 \rightarrow CoO + H_2O + CO_2 \qquad [1]$$

$$CoO + C_2H_4 \rightarrow Co + H_2O + CO_2 \qquad [2]$$

$$Co + H_2O \rightarrow H_2 + CoO \qquad [3]$$

$$Co + CO_2 \rightarrow CO + CoO \qquad [4]$$

$$H_2 + CoO \rightarrow Co + H_2O \qquad [5]$$

$$CO + CoO \rightarrow Co + CO_2 \qquad [6]$$

Reactions [1] and [2] give the first- and second-stage reductions of Co_3O_4, respectively. Hence, a sharp increase in the amount of unreacted ethylene was found between the two stages, i.e., in the valley. When some Co began to form, reactions [3] and [4] started; soon after, reactions [5] and [6] also began. These reactions continued until all the ethoxyl groups were completely decomposed. Therefore, CO and H_2 were detected in the gas phase due to reactions [3] and [4] at the second stage of cobalt reduction.

The DTG curves of the Co/SiO_2 catalysts under H_2 flow are shown in Fig. 8. All samples exhibit a major peak located at 250°C and a shoulder at 235°C. Because a large quantity of water was produced as indicated by their mass spectra, these two peaks represent the reduction of Co_3O_4 by H_2. This agrees well with the reported two-stage reduction characteristic of Co_3O_4 (23). Another weak peak located at 480°C with water formation was also observed for all samples. This peak was attributed to a less reducible cobalt species, probably a $Co{-}SiO_2$ surface compound (12). One additional weight loss peak at 550°C was present on the DTG curves of CoSi500E and CoSi1000E that was also present in the corresponding curves for Si500E and Si1000E, suggesting the contribution of ethoxyl groups. This is confirmed by mass spectra in which only methane was observed in the weight loss peak at 550°C (inset in Fig. 8). Here, ethylene from the decomposition of the ethoxyl groups on silica was catalytically hydrogenated into methane on cobalt metal surface. Methane was also detected in the weight loss peak at 250°C, supporting the above-mentioned assumption of the presence of ethoxyl groups or carbon species on Co_3O_4. The quantitative results of TG are given in Table 4. The reduction of cobalt oxides to Co is nearly complete after reduction at 800°C for all samples based on the weight gain on reoxidation at 400°C. Above 90% of cobalt oxide was reduced to Co below 400°C. The 480°C peak contained only 3% of cobalt oxide for CoSi500H and CoSi1000H. More less-reducible cobalt oxides were found in CoSi500E (8%) and CoSi1000E (6%). In particular, 6% of cobalt oxide in CoSi500E was reduced only in the temperature range 600–800°C, indicating the formation of cobalt silicate in this catalyst. It was reported that an impregnation solution of higher pH favors

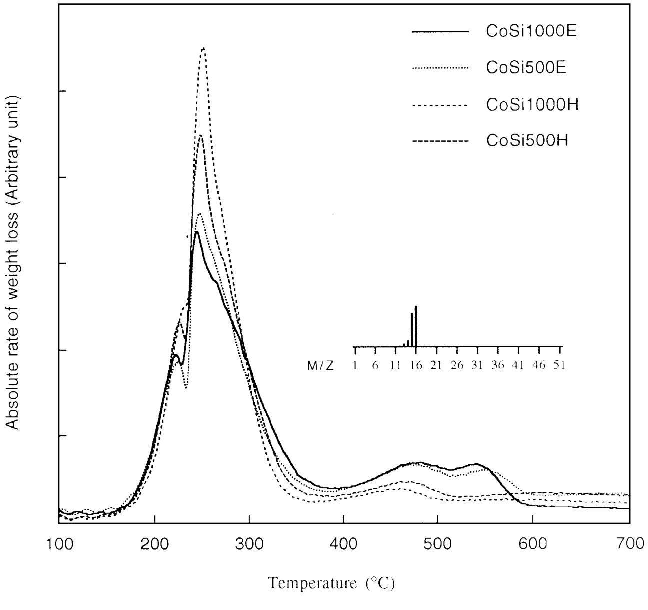

FIG. 8. DTG curves of the Co/SiO_2 catalysts obtained in H_2 flow. The inserted mass spectra were taken at the weight loss peak at 550°C in the DTG curve of CoSi1000E.

TABLE 4

Weight Loss and Extent of Reduction during Temperature-Programmed Reduction for Various 6% Co/SiO_2

	Weight loss (%)		
Sample	250°C peak	480°C peak	% Reduction at 800°C[a]
CoSi1000E	1.92 (1.90)[b] (94)[c]	0.68 (0.13)[b] (6)[c]	100
CoSi500E	1.83 (1.83)[b] (91)[c]	0.54 (0.04)[b] (2)[c]	99[d]
CoSi1000H	2.09 (1.95)[b] (97)[c]	0.26 (0.06)[b] (3)[c]	100
CoSi500H	2.05 (1.95)[b] (97)[c]	0.29 (0.07)[b] (3)[c]	100

[a] Extent of reduction was obtained from the weight gain after reoxidation at 400°C.

[b] Values in parentheses are weight losses corrected for dehydration. The portion of weight loss due to dehydration was estimated from weight loss of CoSi1000H in 1% O_2/He for CoSi1000E and CoSi1000H and that of CoSi500H in 1% O_2/He for CoSi500E and CoSi500H in the corresponding temperature range.

[c] Percentage of weight loss in total weight loss (corrected for dehydration).

[d] There is another 6% weight loss at 800°C for Si500E.

the interaction of cobalt with silica (24, 25). Since ethanol is comparatively more basic than water, it is possible that more surface hydroxyl groups interacted with Co(II) in ethanol solution than in aqueous solution, leading to more Co–SiO_2 interaction species in the ethanol-prepared catalysts.

TPR analyses for CoSi1000E further calcined to 600°C in 1% O_2/He and He are shown in Fig. 9. The TPR analysis for CoSi1000E is also shown here for the purpose of comparison. It is noted that the 550°C peak is no longer present after these treatments. For CoSi1000E further calcined in He, the reduction peak located at 240°C also disappeared. Since this reduction peak represents the first reduction stage of Co_3O_4 to CoO, the absence of this peak indicates that the cobalt phase is CoO. This is in line with XRD result that the main cobalt phase is CoO in CoSi1000E(V). Similar results were obtained for CoSi500E. The quantitative results of TPR for all catalysts after further treatment are given in Tables 5 and 6. After these treatments, the percentage of less-reducible cobalt oxide (480°C reduction peak) increased for all catalysts. The increment is independent on the gas for CoSi500H and CoSi1000H; however, calcination to 600°C in He increased the percentage of the cobalt phase in the less-reducible state to 20% for CoSi500E and CoSi1000E. This indicates that CoO is more active

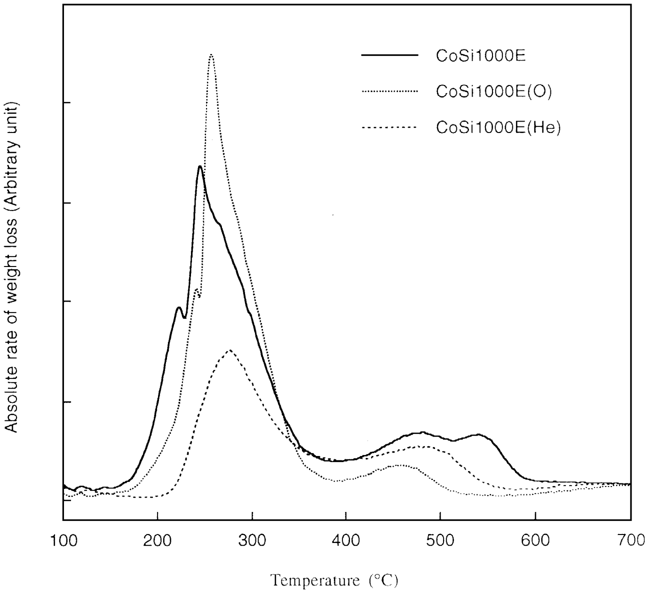

FIG. 9. DTG curves obtained in H_2 flow for CoSi1000E further calcined to 600°C in 1% O_2/He and He.

TABLE 5

Weight Loss and Extent of Reduction during Temperature-Programmed Reduction for Various 6% Co/SiO_2 Heated under 1% O_2/He Flow to 600°C

	Weight loss (%)		
Sample	260°C peak	480°C peak	% Reduction at 800°C[a]
CoSi1000E	1.85 (91)[b]	0.19 (9)[b]	100
CoSi500E	1.73 (87)[b]	0.24 (12)[b]	99
CoSi1000H	1.95 (95)[b]	0.99 (5)[b]	100
CoSi500H	1.91 (94)[b]	0.13 (6)[b]	100

[a] Extent of reduction was obtained from the weight gain after reoxidation at 400°C.

[b] Percentage of weight loss in total weight loss (corrected for dehydration).

TABLE 6

Weight Loss and Extent of Reduction during Temperature-Programmed Reduction for Various 6% Co/SiO_2 Heated under He Flow to 600°C

	Weight loss (%)			
Sample	270°C peak	480°C peak	Reoxidation difference[a]	% Reduction at 800°C[b]
CoSi1000E	0.88 (44)[c]	0.42 (21)[c]	0.70 (35)[d]	100
CoSi500E	1.03 (51)[c]	0.42 (21)[c]	0.53 (27)[d]	99
CoSi1000H	1.95 (95)[c]	0.11 (5)[c]	0 (0)[d]	100
CoSi500H	1.87 (93)[c]	0.15 (7)[c]	0 (0)[d]	100

[a] Difference between the weight gain on reoxidation at 400°C and weight loss on reduction.

[b] Extent of reduction was obtained from the weight gain during reoxidation at 400°C.

[c] Percentage of weight loss in the theoretical weight loss due to reduction of Co_3O_4 to Co.

[d] Percentage of reoxidation difference in the theoretical weight loss due to reduction of Co_3O_4 to Co.

TABLE 7

Amount of Hydrogen Chemisorption and Extent of Reduction for Various 6% Co/SiO_2 Reduced at 400°C

Sample	H_2 amount (μmol/g-cat.)	% Dispersion[c]	% Reduction
CoSi1000H	20.9	9.1	98
CoSi500H	28.7	12.6	97
CoSi1000E	34.8	14.9	99
CoSi500E	34.0	15.7	92
CoSi1000E(O)[a]	26.3	11.4	98
CoSi1000E(V)[b]	24.3	10.8	95

[a] After calcination *in vacuo* at 300°C, sample was further calcined under 1% O_2/He flow at 600°C for 10 min.

[b] After calcination *in vacuo* at 300°C, sample was further calcined *in vacuo* at 600°C for 10 min.

[c] The relative standard deviations for cobalt dispersion measured are less than 10%.

than Co_3O_4 in reacting with silica to form Co–SiO_2 surface species.

Cobalt Dispersions in Reduced Catalysts

The results of hydrogen chemisorption for 6% Co/SiO_2 reduced at 400°C for 8 h are shown in Table 7. In general, the reduction of cobalt oxide to Co was quantitative; only CoSi500E exhibited a slightly lower extent of reduction (92%) in agreement with the results of TG studies. Further calcination of CoSi1000E under 1% O_2/He or *in vacuo* to 600°C gave decreased cobalt metal dispersion. A slight decrease in cobalt reducibility to 95% was also observed for CoSi1000E further calcined *in vacuo* to 600°C.

Both CoSi500E and CoSi1000E have larger amounts of hydrogen chemisorption than the corresponding CoSi500H and CoSi1000H. Cobalt metal dispersion increased from 12.6 to 15.7% for CoSi500 and 9.1 to 14.9% for CoSi1000 when ethanol was employed as an impregnating solvent instead of water. This is consistent with the previous studies in which ethanol solution resulted in better cobalt dispersion (12). The influence of the calcination temperature of the silica support on cobalt metal dispersion depends on the impregnation solution. Similar cobalt dispersion was obtained for CoSi500E and CoSi1000E. In the case of aqueous impregnation, a decrease in cobalt metal dispersion was observed as the calcination temperature increased from 500 to 1000°C. Basically, this trend is parallel to that of Co_3O_4 crystallite size estimated from XRD line broadening. The similarity indicates that the dispersion of cobalt metal is determined primarily by the size of the precursor Co_3O_4. Therefore, the effect of ethanol impregnation on cobalt metal dispersion is attributed to the presence of ethoxyl groups on silica and Co_3O_4 surface which hindered the agglomeration of Co_3O_4 by physically interfering during the thermal decomposition of nitrates. Since ethoxyl groups on silica were stable when CoSi1000E and CoSi500E were heated in H_2 to 400°C, the sintering process of cobalt metal might be obstructed during reduction as well.

CONCLUSIONS

Ethoxyl groups formed on a silica surface when ethanol solution was employed in the impregnation step. The surface density of ethoxyl groups on silica depends on the extent of dehydroxylation of the silica surface and the presence of cobalt nitrate in ethanol. The higher surface density for highly dehydroxylated silica surface is attributed to the formation of more siloxane bridges at 1000°C. The lower surface density in the presence of cobalt nitrate is attributed to the competition of water and cobalt nitrate with ethanol to interact with silica surface.

The temperature and thermal products of the decomposition of ethoxyl groups depend on the feed gas and the presence of Co_3O_4. The products were CO, CO_2, and H_2O (oxidation) in 1% O_2/He, and H_2O, and C_2H_4 (dehydration) in He and H_2. Due to the catalytic effect of Co_3O_4, ethoxyls were completely oxidized into CO_2 and H_2O in 1% O_2/He. Under He, ethoxyls were oxidized to CO, CO_2, and H_2O along with the quantitative reduction of Co_3O_4 to CoO in the catalysts. Under H_2, ethoxyls were catalytically transformed into methane around 550°C on cobalt metal. The similar decomposition temperature range (500–600°C) of ethoxyl groups for the blank silica and the ethanol-prepared catalysts under He and H_2 suggested that the initial product of decomposition of ethoxyl groups is ethylene.

XRD indicates that the main cobalt phase is Co_3O_4 in all samples. TG studies show that there are two kinds of cobalt species in most catalysts; one is more than 90% and shows two-stage reduction under 400°C characteristic of Co_3O_4. The other species which required higher activation temperature is attributed to Co–SiO_2 interaction species. More Co–SiO_2 interaction species were formed when ethanol solutions were employed instead of aqueous solutions; in particular, 6% cobalt was present as cobalt silicate when silica was precalcined at 500°C. Employing ethanol solution significantly decreased Co_3O_4 crystallite size; however, the effect of the calcination temperature of silica on Co_3O_4 crystallite size is not significant.

The smaller Co_3O_4 crystallite size obtained for samples using ethanol as impregnation solvent is attributed to the presence of ethoxyl groups on silica and/or Co_3O_4 surface which hindered the sintering of Co_3O_4 by physically interfering during the thermal decomposition of nitrates. As a result, a higher percentage dispersion of cobalt metal was obtained from reduction of smaller crystallites of Co_3O_4. In addition, further sintering of cobalt metal during reduction might be hindered by ethoxyl groups as well.

ACKNOWLEDGMENT

This work was supported by the National Science Council, Republic of China, under Grant NSC 83-0208-M-006-508.

REFERENCES

1. Withers, H. P., Jr., Eliezer, K. F., and Michell, J. W., *Ind. Eng. Chem. Rev.* **29**, 1807 (1990).
2. Vannice, M. A., *J. Catal.* **50**, 228 (1977).
3. Zotiac, J. M., and Bartholomew, C. H., *J. Catal.* **83**, 107 (1983).
4. Castner, D. G., and Santilli, D. S., *in* "Catalytic Materials" (T. E. Whyte, R. A. Dalla, E. A. Derovane, and R. T. K. Baker, Eds.), ACS Symposium Series 248, p. 39. Am. Chem. Soc., Washington, DC, 1984.
5. Beuther, H., Kibby, C. L., Kobylinski, T. P., and Pannell, R. B., U.S. Patent 4,399,234 (1983).
6. Beuther, H., Kibby, C. L., Kobylinski, T. P., and Pannell, R. B., U.S. Patent 4,605,680 (1986).
7. Payne, V. L., and Mauldin, C. H., U.S. Patent 4,595,703 (1986).
8. Rao, V. U. S., Gormley, R. J., Shamsi, A., Peterick, T. R., Stencel, J. M., Schehl, R. R., Chi, R. D. H., and Obermyrer, R. T., *J. Mol. Catal.* **29**, 271 (1985).
9. Schanke, D., Vada, S., Blekkan, E. A., Hilmen, A. M., Hoff, A., and Holmen, A., *J. Catal.* **156**, 85 (1995).
10. Takeuchi, K., Matsuzaki, T., Aratawa, H., Hanaoka, T., Sugi, Y., and Wei, K. M., *J. Mol. Catal.* **55**, 361 (1989).
11. Lee, W. H., and Bartholomew, C. H., *J. Catal.* **120**, 256 (1989).
12. Ho, S. W., Houalla, M., and Hercules, D. M., *J. Phys. Chem.* **94**, 936 (1990).
13. Guo, S.-L., Arai, M., and Nishiyama, Y., *Appl. Catal.* **65**, 31 (1990).
14. Klug, H. P., and Alexander, L. E., "X-ray Diffraction Procedures," p. 491. Wiley, New York, 1954.
15. Abrams, L., and Allen, A. O., *J. Phys. Chem.* **73**, 2741 (1969).
16. Acosta Saracual, A. R., Pulton, S. K., Vicary, G., and Rochester, C. H., *J. Chem. Soc. Faraday Trans. 1* **78**, 2285 (1982).
17. Nakajima, T., Nameta, H., Mishima, S., Matsuzaki, I., and Tanabe, K., *J. Mater. Chem.* **4**, 853 (1994).
18. Zhuravlev, L. T., *Colloids Surf. A* **74**, 71 (1993).
19. Lygin, V. I., *Kinet. Catal.* **35**, 480 (1994).
20. Boreskov, G. K., *in* "Catalysis, Science and Technology" (J. R. Anderson and M. Boudart, Eds.), Vol. 3, p. 39. Springer, Berlin, 1982.
21. Germain, J. E., "Catalytic Conversion of Hydrocarbons." Academic Press, London, 1969.
22. Busca, G., Guidetti, R., and Lorenzelli, V., *J. Chem. Soc. Faraday Trans.* **86**, 989 (1990).
23. Sexton, B. A., Hughes, A. E., and Turney, T. W., *J. Catal.* **97**, 390 (1986).
24. Puskas, I., Fleisch, T. H., Hall, J. B., Meyers, B. L., and Roginski, R. T., *J. Catal.* **134**, 615 (1992).
25. Ming, H., and Baker, B. G., *Appl. Catal.* **123**, 23 (1995).